
FETREG: PLACENTAL VESSEL SEGMENTATION AND REGISTRATION IN FETOSCOPY CHALLENGE DATASET

Sophia Bano¹, Alessandro Casella^{2,3}, Francisco Vasconcelos¹, Sara Moccia⁴, George Attilakos^{5,8}, Ruwan Wimalasundera^{5,8}, Anna L. David^{5,7,8}, Dario Paladini⁶, Jan Deprest^{7,8}, Elena De Momi³, Leonardo S. Mattos², and Danail Stoyanov¹

¹Wellcome/EPSRC Centre for Interventional and Surgical Sciences(WEISS) and Department of Computer Science, University College London, London, UK

²Department of Advanced Robotics, Istituto Italiano di Tecnologia, Genoa, Italy

³Department of Electronics, Information and Bioengineering, Politecnico di Milano, Milan, Italy

⁴The BioRobotics Institute, Scuola Superiore Sant'Anna, Pisa, Italy

⁵Fetal Medicine Unit, Elizabeth Garrett Anderson Wing, University College London Hospital, London, UK

⁶Department of Fetal and Perinatal Medicine, Istituto "Giannina Gaslini", Genoa, Italy

⁷Department of Development and Regeneration, University Hospital Leuven, Leuven, Belgium

⁸EGA Institute for Women's Health, Faculty of Population Health Sciences, University College London, UK

Correspondance: ¹sophia.bano@ucl.ac.uk

ABSTRACT

Fetoscopy laser photocoagulation is a widely used procedure for the treatment of Twin-to-Twin Transfusion Syndrome (TTTS), that occur in mono-chorionic multiple pregnancies due to placental vascular anastomoses. This procedure is particularly challenging due to limited field of view, poor manoeuvrability of the fetoscope, poor visibility due to fluid turbidity, variability in light source, and unusual position of the placenta. This may lead to increased procedural time and incomplete ablation, resulting in persistent TTTS. Computer-assisted intervention may help overcome these challenges by expanding the fetoscopic field of view through video mosaicking and providing better visualization of the vessel network. However, the research and development in this domain remain limited due to unavailability of high-quality data to encode the intra- and inter-procedure variability. Through the *Fetoscopic Placental Vessel Segmentation and Registration (FetReg)* challenge, we present a large-scale multi-centre dataset for the development of generalized and robust semantic segmentation and video mosaicking algorithms for the fetal environment with a focus on creating drift-free mosaics from long duration fetoscopy videos. In this paper, we provide an overview of the FetReg dataset, challenge tasks, evaluation metrics and baseline methods for both segmentation and registration. Baseline methods results on the FetReg dataset shows that our dataset poses interesting challenges, offering large opportunity for the creation of novel methods and models through a community effort initiative guided by the FetReg challenge.

Keywords Fetoscopic video · Placental semantic segmentation · Image registration · Video mosaicking · Twin-to-twin transfusion syndrome

1 Introduction

Twin-to-twin Transfusion Syndrome (TTTS) is a rare complication of monochorionic twin pregnancies, affecting 10-15% of monochorionic diamniotic pregnancies. TTTS is characterized by the development of an unbalanced and chronic blood transfer from one twin (the donor twin), to the other (the recipient twin), through placental anastomoses [1]. This shared circulation causes profound fetal hemodynamic unbalance and consequently severe growth restriction, cardiovascular dysfunction, profound anaemia, hypovolaemic shock, circulatory collapse, hypoxic brain damage and death of one or both twins [2].

In 2004, a randomized, controlled trial demonstrated that fetoscopic laser ablation of placental anastomoses in TTTS resulted in a higher survival rate for at least one twin compared with other treatments, such as serial amnioreduction. Laser ablation further showed lower incidence of complications, such as cystic periventricular leukomalacia and neurologic complications [3, 4]. The reported mortality for untreated TTTS was 90% [5], after the implementation of laser therapy overall survival is around 63%, and survival of at least one twin can reach 76% of pregnancies [6]. A comprehensive description of all the steps that have led to consider laser surgery for coagulation of placental anastomoses the treatment of choice for TTTS can be found in [7].

Two types of laser ablation were studied in the past. The first (i) method is to laser coagulate all vessels that appear on fetoscopic examination to be an anastomosis. This is a non-reproducible and operator-dependent technique, which preserves placental function but which can miss important anastomoses. The second (ii) method, which reduces placental damage over (i), is laser coagulation of all vessels emerging from the amniotic membrane insertion, which relies on the assumption that all of these are vascular anastomoses [8]. Today, the recognized elective treatment is the selective laser photocoagulation of communicating vessels originating in the donor's placental territory. This method requires precise identification and laser ablation of placental vascular anastomoses. It relies on the classification of anastomoses in arterio-venous (from donor to recipient, AVDR, or from recipient to donor, AVR), arterio-arterial (AA) or veno-venous (VV), and may distribute themselves following a certain pattern on the placenta. Recent researches have identified that the sequence in which these anastomoses are treated with the laser could result in further hypotension of the donor twin, with increased risks of complications and fetal demise [9].

However, significant complication or failures were recorded in both techniques, the reason being that tiny anastomoses might be overlooked because flattened on the placental surface by the high pressure in the recipient's sac. Therefore, the Solomon technique was introduced [10] and now has become the gold standard in those cases in which it can be technically achieved. This technique consists in drawing a coagulation line connecting all the sites in which anastomoses had been coagulated after the first selective ablation round.

Despite all the advancements in instrumentation and imaging for TTTS [11], residual anastomoses still represent a major complication in monochorionic placentas treated with fetoscopic laser surgery [12]. This may be explained considering the challenges in identifying anastomoses in conditions of poor visibility and constrained maneuverability of the fetoscope, especially in the presence of anterior placenta due to the unfavourable viewing angle. In this complex scenario, Computer-Assisted Intervention and Surgical Data Science methodologies may be exploited to provide surgeons with context awareness and decision support. However, the research in this field is still at its early stages and several challenges still have to be tackled [13].

To foster research in this field, we organized the **FetReg: Placental Vessel Segmentation and Registration in Fetoscopy**¹ inside the EndoVis MICCAI Grand Challenge². This paper describes the FetReg Challenge in terms of tasks, datasets and evaluation procedures.

¹FetReg2021 Challenge website: <https://fetreg2021.grand-challenge.org/>

²MICCAI EndoVis Challenge website: <https://endovis.grand-challenge.org/>

2 Literature Review

In this section, we provide a short overview of current literature in the field of placenta vessel segmentation and mosaicking.

2.1 Placenta Vessel Segmentation

The Surgical Data Science [14] community is working towards developing computer-assisted algorithms to perform intra-operative tissue segmentation. However, Surgical Data Science approaches for fetal image segmentation, including inter-fetus (twin) membrane and placenta-vessel segmentation, have only been marginally explored. A number of approaches have been proposed for inter-twin membrane segmentation from in-vivo placenta [15, 16], but vessel segmentation is currently covering a larger space in the literature. Vessel segmentation is used both to directly provide guidance to the surgeon and as a prior to perform mosaicking for field-of-view expansion. Examples include [17, 18]. In [17], a shallow U-Net architecture is proposed to perform patch-based vessel segmentation from intra-operative fetoscopic frames. U-Net is also used in [19], where vessel probability maps are exploited to perform image mosaicking.

Despite the promising results, limitations still exist which hamper the translation of the proposed methodology in the clinical practice. Besides the development of advanced algorithms, a major effort is needed to collect large, high-quality, multi-centre datasets, which are currently not available to the research community. Having such multi-centre datasets is crucial with a view to attenuate the well-known problem of covariance shift and develop robust and generalizable algorithms.

2.2 Video Mosaicking

Several Surgical Data Science approaches have been proposed for fetoscopic mosaicking in the years. A first distinction can be made between approaches that rely on image information only and those that exploit additional hardware, such as [20] that rely on electromagnetic tracking. Among methods that exploit only information from the fetoscope, some researchers have proposed indirect registration methods based on extraction and matching of image features [21, 22]. These approaches, however, have only been validated on synthetic phantom or ex-vivo placental sequences where the imaging resolution, visual quality and appearance are vastly different from in-vivo placental imaging. On the other hand, direct registration methods [23] minimize photometric consistency between frames and have been more successful at dealing with in-vivo fetoscopy data. More recently, deep learning algorithms have been proposed, both for homography estimation [18, 19] and detection of stable regions as a prior for frame registration [24]. These approaches are validated on in-vivo [18, 19] or an underwater phantom setting [24]. In [19], it is shown that placental vessels provide unique landmarks which help in overcoming visibility challenges in in-vivo placental imaging. As a result, the use of segmented vessel maps for consecutive frame registration generate reliable mosaics.

Robotics has shown the potential to improve stability of the imaging device by providing precise control of the fetoscopy instrument [25]. Efforts have also been made towards the design of a robotic multimodal endoscope that includes an optical ultrasound and white light stereo camera [26]. This endoscope has shown to provide improved visualization in an in-lab phantom experiment. Due to the limited form-factor of the clinically approved fetoscope, these solutions are not yet applicable in clinical settings.

While promising results have been achieved for mosaicking from short video sequences, long-term mapping still remains an open challenge. This is because of the intra- and inter-case variability in each procedure, dynamically challenging non-planar views, poor visibility, texture paucity, low resolution and occlusion due to the presence of fetus and ablation tool in the field-of-view.

3 Challenge Tasks

The *FetReg challenge* aims to advance the current state-of-the-art in placental vessel segmentation and mosaicking [19] by providing a benchmark multi-centre large-scale dataset that captures variability across different patients and different clinical institutions. The participants are required to complete two sub-tasks on the provided dataset:

- **Task 1: Placental semantic segmentation:** The participants are required to segment four classes, namely, background, vessels, tool (ablation instrument) and fetus. This task will be evaluated on an unseen test data that is independent of the training data videos. The aim is to assess the generalization capability of the trained segmentation model on unseen fetoscopic video frames. The evaluation metric for the segmentation task is provided in Section 5.1.
- **Task 2: Registration for Mosaicking:** The participants are required to perform registration of consecutive frames to create an expanded field-of-view image of the fetoscopic environment. The task will be evaluated on unseen video clips extracted from fetoscopic procedure videos which are not part of the training data. The aim is to assess the robustness and performance of the participant’s registration method for creating a drift-free mosaic from unseen data. Details of the evaluation metric for the registration task are provided in Section 6.2.

4 Dataset Collection

The *FetReg* dataset is unique as it is the first large-scale fetoscopic video dataset of 18 different procedures. The videos contained in this dataset are collected from three fetal surgery centres across Europe, namely,

- Fetal Medicine Unit, University College London Hospital (UCLH), London, UK,
- Department of Fetal and Perinatal Medicine, Istituto "Giannina Gaslini", Genoa, Italy,
- Department of Development and Regeneration, University Hospital Leuven, Leuven, Belgium.

Alongside capturing the intra-case and inter-case variability, the multi-centre data collection allowed capturing the variability that arises due to different clinical settings and imaging equipment at different clinical sites. At UCLH, the data collection was carried out as part of the GIFT-SURG³ project. The requirement for formal ethical approval was waived as the data were fully anonymized in the corresponding clinical centres before being transferred to the organizers of the *FetReg* challenge. The fully anonymized fetoscopic data used in this challenge will be published for research and educational purposes after the challenge⁴.

4.1 Segmentation Dataset Description

Fetoscopy videos acquired from the three different fetal medicine centres are first decomposed into frames and excess black background is cropped to obtain squared images capturing mainly the fetoscope field-of-view. From each video a subset of 100-150 non-overlapping informative frames was selected and manually annotated. All pixels in each image are labelled with background (0), placental vessel (1), ablation tool (2) or fetus class (3). There is no overlap between the segmentation labels, hence all labels are mutually exclusive.

Annotations were performed by four academic researchers and staff members with a background in fetoscopic imaging. Additionally, annotation services were obtained from Humans in the Loop (HITL)⁵ for a subset of videos. HITL is an award-winning social enterprise founded in 2017 who provides annotations using skilled workers displaced by conflict with the vision to connect the conflict-affected communities to digital work. All the annotations were further verified

³GIFT-Surg project: <https://www.gift-surg.ac.uk/>

⁴FetReg data is currently available only to the EndoVis2021 participants upon signing the EndoVis2021 rule agreement. The public data release is subject to the publication of the joint journal article on the challenge results and data analysis.

⁵Humans in the Loop: <https://humansintheloop.org/>

Table 1: Summary of the challenge dataset. For each video, image resolution, number of annotated frames (for the segmentation task), occurrence of each class per frame and average number of pixels presence per class per frame are presented. For the registration task, number of unlabelled frames in each video clip are provided. Key: BG - background.

Sr.	Video name	Image Resolution (pixels)	No. of Labelled frames	Occurrence (frame)			Occurrence (Avg. pixels)			Unlabelled clips # frames	
				Vessel	Tool	Fetus	BG	Vessel	Tool		Fetus
1.	Video001	470 × 470	152	152	21	11	196463	21493	1462	1482	346
2.	Video002	540 × 540	153	153	35	1	271564	16989	3019	27	259
3.	Video003	550 × 550	117	117	52	32	260909	27962	3912	9716	541
4.	Video004	480 × 480	100	100	21	18	212542	14988	1063	1806	388
5.	Video005	500 × 500	100	100	35	30	203372	34350	2244	10034	722
6.	Video006	450 × 450	100	100	49	4	171684	28384	1779	653	452
7.	Video007	640 × 640	140	140	30	3	366177	37703	4669	1052	316
8.	Video008	720 × 720	110	105	80	34	465524	28049	13098	11729	295
9.	Video009	660 × 660	105	104	40	14	353721	68621	7762	5496	265
10.	Video011	380 × 380	100	100	7	37	128636	8959	184	6621	424
11.	Video013	680 × 680	124	124	54	21	411713	36907	8085	5695	247
12.	Video014	720 × 720	110	110	54	14	464115	42714	6223	5348	469
13.	Video016	380 × 380	100	100	16	20	129888	11331	448	2734	593
14.	Video017	400 × 400	100	97	20	3	151143	7625	753	479	490
15.	Video018	400 × 400	100	100	26	11	139530	15935	1503	3032	352
16.	Video019	720 × 720	149	149	15	31	470209	38513	1676	8002	265
17.	Video022	400 × 400	100	100	12	1	138097	21000	650	253	348
18.	Video023	320 × 320	100	92	14	8	94942	6256	375	828	639
All videos			2060	2043	581	293	4630229	467779	58905	74987	7411

by two fetal medicine specialists who confirmed the correctness and consistency of the labels. The publicly available Supervisely⁶ platform was used for annotating the dataset.

FetReg dataset for the segmentation task contains 2060 annotated images from 18 different in-vivo TTTS fetoscopic surgeries. Table 1 summarizes the segmentation dataset. Note that the frames present different resolutions as the fetoscopic videos are captured at different centres with different facilities (e.g., device, light scope). From the occurrences of the classes in Table 1, it can be observed that the dataset is highly unbalanced, the *Vessel* is the most frequent class while *Tool* and *Fetus* are presented only in a small subset of images corresponding to 28% of the dataset. Fig. 1 and Fig. 2 show some representative annotated frames images from each video. Note that the frame appearance and quality changes in each video due to the large variation in intra-operative environment among different cases. Amniotic fluid turbidity resulting in poor visibility, artefacts introduced due to spotlight light source and reddish reflection introduced by the laser tool, low resolution, texture paucity, non-planar views due to anterior placenta imaging, are some of the major factors that contribute to increase the variability in the data. Large intra-case variation can also be observed from these representative images. All these factors contribute towards limiting the performance of the existing placental image segmentation and registration methods [19, 18, 27].

The *FetReg* challenge provides an opportunity to make advancements in the current literature by designing and contributing novel segmentation and registration methods that are robust even in the presence of the above-mentioned challenges.

⁶Supervisely: a web-based annotation platform: <https://supervise.ly/>

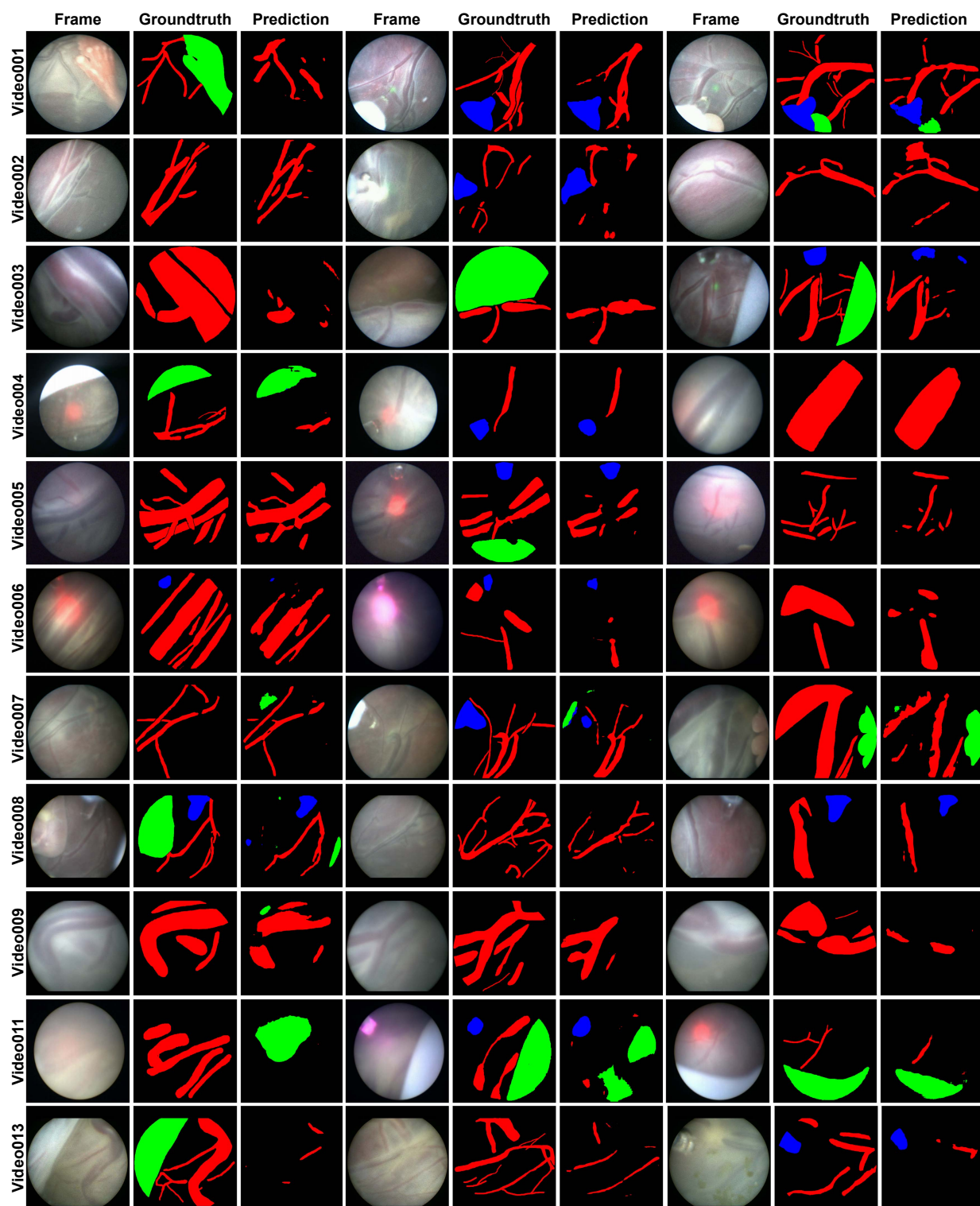


Figure 1: Representative images along with the segmentation annotations (Groundtruth) and baseline segmentation output (Prediction) for Video001, 002, 003, 004, 005, 006, 007, 008 and 009 videos. Background (black), vessel (red), tool (blue) and fetus (green) labels are shown. Observe the intra- and inter-case variability in the videos.

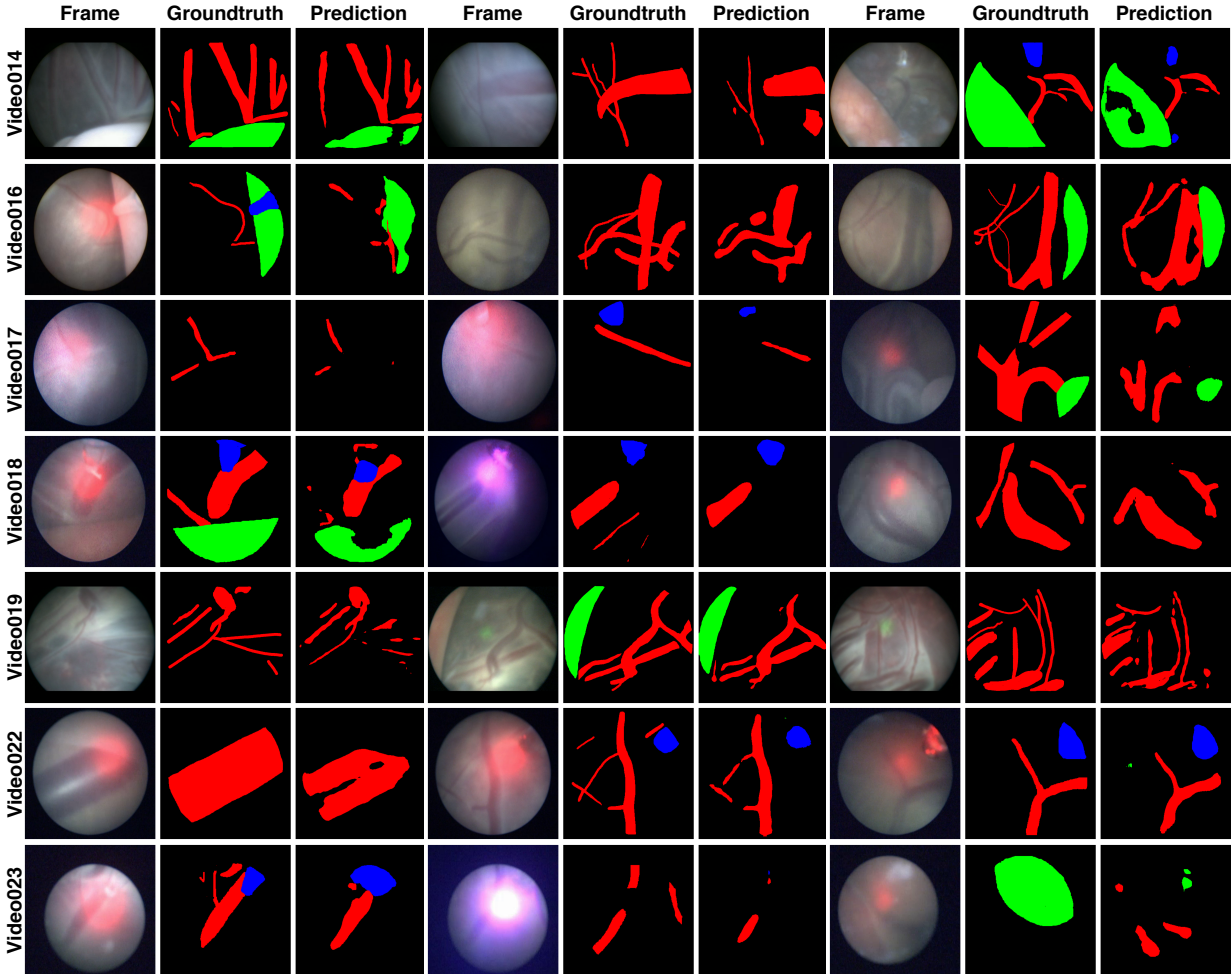


Figure 2: Representative images along with the segmentation annotations (Groundtruth) and baseline segmentation output (Prediction) for Video014, 016, 017, 018, 019, 022 and 023 videos. Background (black), vessel (red), tool (blue) and fetus (green) labels are shown. Observe the intra- and inter-case variability in the videos.

4.2 Registration Dataset Description

Average duration of the TTTS fetoscopic surgery is approximately 30 minutes. Not all fetoscopic frames are suitable for frame registration and mosaicking. This is because of the presence of fetuses, laser ablation fibre and working channel port which can occlude the field-of-view of the fetoscope. Frame registration and mosaicking is only required in occlusion-free video segments that capture the surface of the placenta [28] as these are the segments in which the surgeon is exploring the intraoperative environment to identify abnormal vascular connections. Expanding the field-of-view through mosaicking in these video segments can facilitate the procedure by providing better visualization of the environment.

For the registration and mosaicking task, we have provided one video clip per video for all 18 procedures in our dataset. These frames are not annotated with segmentation labels. The number of frames in each video clip is reported in Table 1. Representative frames at every 2 seconds from the 18 video clips are shown in Figure 3. Observe the variability in the appearance, lighting conditions and image quality in all video clips. Even though there is no noticeable deformation in fetoscopic videos, which is usually thought to occur due to breathing motion, the views can be non-planar as the

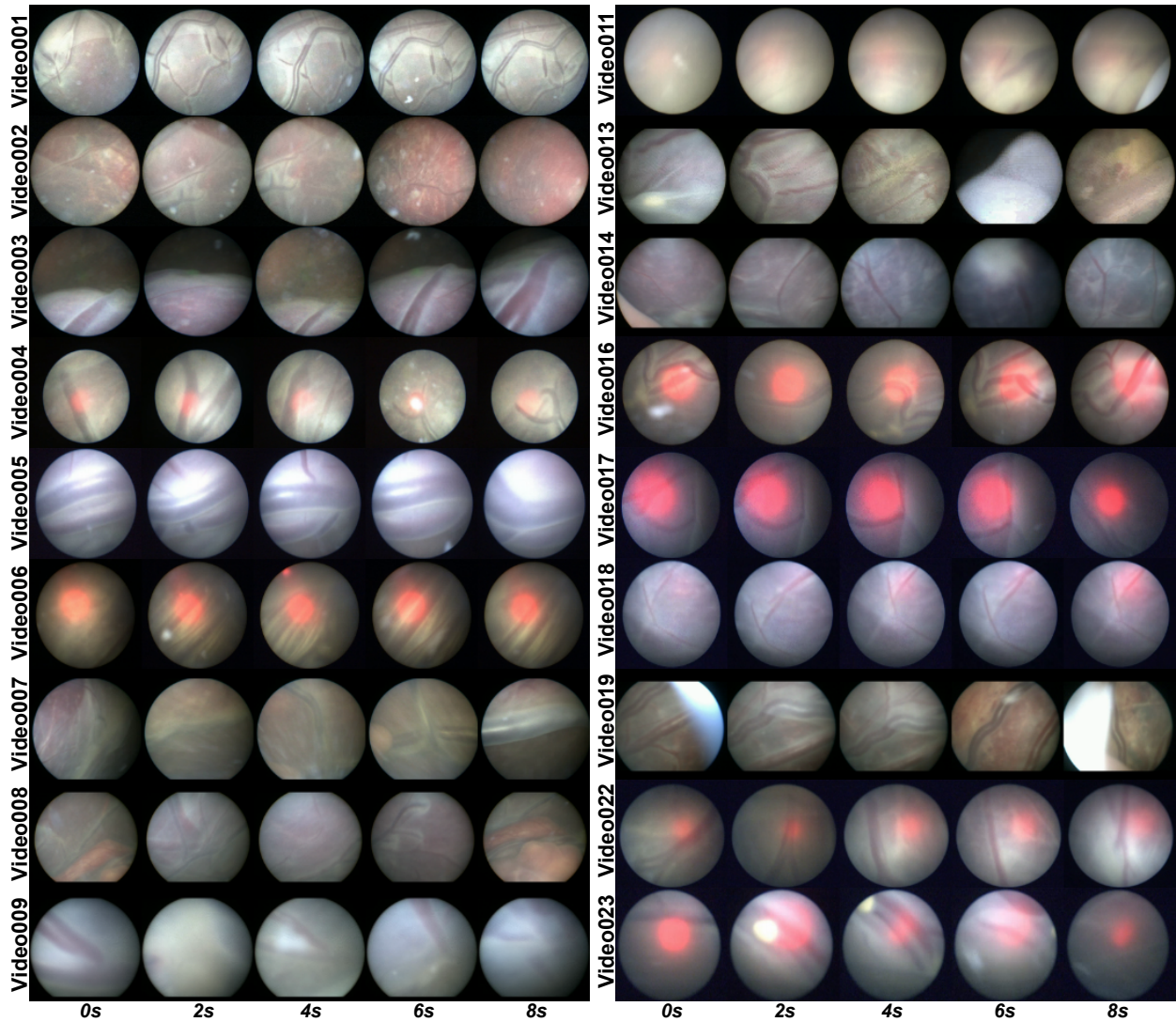


Figure 3: Representative frames at every 2 seconds from the 18 video clips. These clips are unannotated and are released for the registration and mosaicking task. Number of frames in each clip are mentioned in Table 1.

placenta can be anterior or posterior. Moreover, there is no groundtruth camera motion and scene geometry that can be used to evaluate video registration approaches for in-vivo fetoscopy. In Section 6.2, we detail how this challenge is addressed with an evaluation metric that is correlated with good quality, consistent, and complete mosaics [19].

5 Segmentation

Segmenting intraoperative fetoscopy images mainly involves blood vessels, fetuses (and related fetal parts) and surgical (laser) tools. Segmenting these structures can support indirect registration methods to accomplish the mosaicking task. Hence, the research community has been working to develop algorithms for robust and accurate segmentation, with a particular focus on vessel segmentation.

Obtaining an accurate segmentation is challenging due to homogeneous texture of the tissues and reduced visibility within the amniotic sac (small field-of-view of the fetoscope, turbidity of the amniotic fluid). The quality of fetoscopic images is further degraded by the presence of occlusions (laser fibre, fetuses and particles) and light reflections. In anterior placental procedures, where the 30° fetoscope is used, the field-of-view is further reduced due to the view angle between the camera and the placenta surface.

In *FetReg*, placental semantic segmentation is treated as a multi-class problem (refer to Sec. 4.1).

5.1 Segmentation metric

For evaluating the performance of segmentation models, we compute for each frame provided in the test set the Mean Intersection over Union (*IoU*) per class between the prediction and the manually annotated groundtruth.

$$IoU = \frac{TP}{(TP + FP + FN)} \quad (1)$$

where *TP* are the correctly classified pixels belonging to a class, *FP* are the pixels incorrectly predicted as in that specific class and *FN* are the pixels in that class incorrectly classified as not belonging to it.

5.2 Baseline method

As the baseline model for analysing the *FetReg* segmentation sub-task, we trained a U-Net [29] with ResNet50 [30] backbone. U-Net was selected as the baseline as it is the most commonly used network for biomedical imaging segmentation. Softmax activation was used at the final layer of the network (considering the multi-class nature of the segmentation dataset). Cross entropy loss was computed and backpropagated during training.

5.3 Experimental Setup

Our baseline model was trained for 300 epochs on the dataset provided for Task 1. The performance for all patients is evaluated by training the model using the cross-fold validation scheme shown in Table 2. We created 6 folds, where each fold contained 3 procedures, with the aim to preserve as much variability as possible for each fold while keeping the number of samples in each fold approximately balanced. During training, the images were resized to 448×448 pixels to reduce the probability of getting unannotated crops when compared to the original size, keeping negligible the loss of information introduced by resampling. To perform data augmentation, at each iteration step, a patch of 256×256 pixels was extracted at a random position in the image. Each of the extracted patches was augmented by applying a random rotation in range $(-45^\circ, +45^\circ)$, horizontal and vertical flip, scaling with a factor in the range of $(-20\%, +20\%)$ and random variation in brightness $(-20\%, +20\%)$ and contrast $(-10\%, +10\%)$. Segmentation results on the dataset released for Task 1 were obtained by patch-wise inference using 256×256 pixels patches with stride=8.

5.4 Results and Discussion

Table 2 shows the cross-validation results over each fold and individual videos reporting the per-class and overall mIOU values. Predicted segmentation masks for some representative images for each video are shown in Fig. 1 and Fig. 2.

For vessel segmentation, U-Net with ResNet50 backbone achieved a Mean *IoU* 0.7892. From Fig. 1 and Fig. 2, it can be observed that overall vessel segmentation gave promising results. In challenging cases, such as when the laser glow was extremely strong (Video023), the vessels were not segmented properly. Another issue was found in the presence of vessels with different morphology and contrast with respect to the training set (e.g., Video003) that led to inaccurate vessel segmentation.

The class imbalance of the dataset, which was discussed in Sec.4.1, impacted on identification of the tool (Mean *IoU* 0.7637) and the fetus (Mean *IoU* 0.7522). As shown in Video001, Video003, Video005, Video008 and Video023, the

Table 2: Results of segmentation for the Task 1 dataset. Mean IoU for each class over each video and, in the last row, the average mean IoU per class are reported. Key: BG-background.

Video	Class				Overall per video	Fold	Images per fold	Class				Overall per fold
	BG	Vessel	Tool	Fetus				BG	Vessel	Tool	Fetus	
Video001	0.83	0.85	0.69	0.74	0.64	1	352	0.80	0.83	0.64	0.74	0.61
Video006	0.67	0.67	0.74	0.76	0.58							
Video016	0.80	0.83	0.64	0.74	0.60							
Video002	0.78	0.79	0.80	0.53	0.56	2	353	0.80	0.81	0.83	0.78	0.69
Video011	0.75	0.72	0.73	0.83	0.64							
Video018	0.80	0.81	0.83	0.78	0.71							
Video004	0.80	0.80	0.72	0.80	0.66	3	349	0.76	0.78	0.79	0.55	0.65
Video019	0.81	0.81	0.64	0.85	0.65							
Video023	0.76	0.78	0.79	0.55	0.56							
Video003	0.79	0.81	0.72	0.79	0.66	4	327	0.82	0.82	0.80	0.93	0.66
Video005	0.71	0.77	0.79	0.56	0.56							
Video014	0.82	0.82	0.80	0.93	0.78							
Video007	0.78	0.77	0.84	0.72	0.66	5	350	0.78	0.81	0.85	0.54	0.67
Video008	0.78	0.76	0.75	0.85	0.68							
Video022	0.78	0.81	0.85	0.54	0.60							
Video009	0.80	0.80	0.80	0.73	0.66	6	329	0.66	0.66	0.73	0.57	0.58
Video013	0.72	0.77	0.75	0.50	0.50							
Video017	0.66	0.66	0.73	0.57	0.48							
per class	0.78	0.79	0.76	0.75								

fetus in the scene was not identified at all. It can be clearly observed that the different shades on the fetus causes holes in the segmentation masks as in Video011, Video014 and Video018. The tool was correctly identified, even if not accurately segmented, in all videos. This is explainable considering the regular structure of tool.

With the *FetReg* challenge, we aim to dramatically improve these performances, fostering breakthroughs in deep learning to provide context awareness to fetoscopy surgeons.

6 Registration and Mosaicking

6.1 Problem Formulation

In its most general form, the registration of fetoscopic placental images is a complex non-linear mapping that involves not only dealing with changes in camera perspective but also lens distortion, fluid light refraction, irregular placental shape, and outlier occlusions (laser tool, fetus, floating particles). To further the problem complexity, calibrating the fetoscopic camera parameters before an in-vivo procedure is unfeasible not only due to the strict workflow in the operating room but also because some camera parameters change dynamically when focus is adjusted or the lens physically rotates.

Throughout the fetoscopic registration literature, most of these complexities have been ignored in favour of simple model approximations that render the problem tractable. Typically, a linear mapping between 2D homogeneous image coordinates is considered (i.e. a homography). This assumes absence of lens distortion and light refraction, and that the visualized scene is either fully planar or locally-planar. For algorithm stability and convergence, it is common to further constrain the problem to an affine registration (6 parameters), which is a sub-set of a general homography (8 parameters). In the context of this challenge we define the registration between fetoscopic frames to be of a general homography mapping, although further constraints or simplifications can be considered by participants as they see fit.

We assume that a registration algorithm receives as input a set of $N \in \{2, 3, \dots, N\}$ consecutive image frames from a video $\{\mathcal{I}_1, \mathcal{I}_2, \dots, \mathcal{I}_N\}$ and outputs a set of $N - 1$ incremental (pairwise) homography transformations $\{H_1, H_2, \dots, H_{N-1}\}$. Each homography H_i is a 3×3 matrix that linearly maps the homogeneous coordinates of a 2D point $\mathbf{p}_i = (x_i \ y_i \ 1)^\top$ in image \mathcal{I}_i to its corresponding point $\mathbf{p}_{i+1} = (x_{i+1} \ y_{i+1} \ 1)^\top$ in image \mathcal{I}_{i+1} :

$$\mathbf{p}_{i+1} \sim H_i \mathbf{p}_i \quad (2)$$

where \sim denotes equality up to a scale factor. Mapping points beyond consecutive frames is achieved with chained homography multiplication

$$\mathbf{p}_{i+n} \sim H_{i \rightarrow i+n} \mathbf{p}_i, \quad H_{i \rightarrow i+n} \sim H_{i+n} \dots H_{i+2} H_{i+1} H_i \quad (3)$$

We can also warp an entire image \mathcal{I}_i so that it is aligned with an image \mathcal{I}_{i+n} by re-mapping and interpolating every pixel

$$\mathcal{I}_{i \rightarrow i+n} = w(\mathcal{I}_i, H_{i \rightarrow i+n}) \quad (4)$$

There are multiple ways to define the warping function $w(\mathcal{I}_i, H_{i \rightarrow i+n})$, depending on the interpolation method. In this paper, we assume bilinear interpolation, which is the default option of the OpenCV function `cv2.warpPerspective()`.

6.2 Registration metric

Given N consecutive frames and a set of $N - 1$ homographies $\{H_1, H_2, \dots, H_{N-1}\}$, we can evaluate their consistency. We use the term consistency rather than accuracy since in the context of this challenge there are no groundtruth homographies. The ultimate clinical goal of fetoscopic registration is to generate consistent, comprehensible and complete mosaics that map the placental surface and guide the surgeon. We therefore consider for evaluation the registration consistency between pairs of non-consecutive frames that have a large overlap in field of view and present a clear view of the placental surface. The list of overlapping frame pairs on the test data can thus be considered as the *groundtruth* information that is not disclosed to participants until challenge completion.

The overwhelming majority of overlapping frame pairs will be temporally close to each other, but can also include distant frames that revisit the same part of the scene. For algorithm evaluation, these frame pairs will be selected so that they always represent a clear view of the placental surface (no heavy occlusions) and their field of view overlapping area is always larger than 25%. In this paper, we will present consistency results for all image pairs that are 5 frames apart in a video (very large overlap), replicating the evaluation metric in [19].

Consider a source image \mathcal{I}_i , a target image \mathcal{I}_{i+n} , and a homography transformation $H_{i \rightarrow i+n}$ between them. We define the consistency between these two images as

$$s_{i \rightarrow i+n} = \text{sim} \left(w(\tilde{\mathcal{I}}_i, H_{i \rightarrow i+n}), \tilde{\mathcal{I}}_{i+n} \right) \quad (5)$$

where $\text{sim}()$ is an image similarity metric that is computed based on target image and warped source image, and $\tilde{\mathcal{I}}$ is a smoothed version of the image \mathcal{I} . We will define both these operations next:

- **Smoothing:** $\tilde{\mathcal{I}}$ is obtained by applying a 9×9 Gaussian filter with standard deviation of 2 to the original image \mathcal{I} . This is fundamental to make the similarity metric robust to small outlier (e.g. particles) and image discretization artefacts.
- **Similarity:** We start by determining the overlap region between the target $\tilde{\mathcal{I}}$ and the warped source $w(\tilde{\mathcal{I}}_i, H_{i \rightarrow i+n})$, taking into account their circular edges. If the overlap contains less than 25% of $\tilde{\mathcal{I}}$, we consider that the registration failed as there will be no such cases in the evaluation pool. A rectangular crop is fit to the overlap, and the structural similarity index metric (SSIM) is calculated between the image pairs after having been smoothed, warped, and cropped.

6.3 Baseline method

In this paper, we report the results obtained from the vessel map registration and mosaicking method reported in [19] when applied to the unannotated 18 video clips provided as training set for Task 2. Vessel segmentation maps from consecutive frames are aligned by applying pyramidal Lucas-Kanade registration based direct registration approach. This approach minimizes the photometric loss between a fixed and a warped moving image. Since fetoscopic images have a circular field-of-view, the registration is performed using a circular mask that allows only analysing the flow field within the fetoscopic image field-of-view. Sequential registrations are then blended using the chain rule (eq. 3) into a single large field-of-view image.

6.4 Results and Discussion

Qualitative and quantitative results for mosaicking are shown in Figures 4 to 6. The mosaics of the vessel maps, RGB images and the evaluation metric plot for very pair of images 5 frames apart in a sequence are shown for all 18 video clips. For better visualization, mosaics are only displayed for the frames marked in red in the evaluation plots. For all 18 unannotated unseen video clips, the vessel maps are obtained through 6-fold cross-validation (presented in Sec. 5.3). It can be observed from these results that for sequences with clearly visible vessels (e.g. Video001, Video002, Video007, Video008), the obtained mosaics are consistent with a high evaluation score in the visualized video segment. There are some clips containing either heavy occlusions (Video008, Video013, Video019) or highly skewed views of the placenta (e.g. Video003) which can be observed in Fig. 3). Moreover, in frames with lack of texture and no visible vessels, our registration approach becomes invalid since it entirely relies on vessel segmentations. These issues cause registration to occasionally fail and therefore our baseline is often unable to reconstruct a continuous, smooth mosaic containing the entirety of a clip.

While vessel-based registration facilitated in dramatically improving results over other existing approaches and helped in overcoming some visibility related challenges, fully robust mosaicking in fetoscopic videos still remains an open challenge. With the *FetReg* challenge, we aim to open new frontiers in designing generalized models for fetoscopic videos that can overcome most of the associated challenges and can create consistent and drift-free mosaic for longer duration video clips.

Acknowledgements This work was supported by the Wellcome/EPSRC Centre for Interventional and Surgical Sciences (WEISS) at UCL (203145Z/16/Z), EPSRC (EP/P027938/1, EP/R004080/1,NS/A000027/1), the H2020 FET (GA 863146) and Wellcome [WT101957]. Danail Stoyanov is supported by a Royal Academy of Engineering Chair in Emerging Technologies (CiET1819/2/36) and an EPSRC Early Career Research Fellowship (EP/P012841/1).

7 Conclusion

In this paper, we presented a large multi-centre fetoscopic dataset extracted from 18 different TTTS laser therapy procedures, which is being proposed for the FetReg Challenge. While there has been recent progress in developing computer-assisted guidance algorithms for this procedure using segmentation and mosaicking techniques, none of them has been tested on such a large scale dataset to date. Results from state-of-the-art techniques for both vessel segmentation and sequential frame registration [19] on this dataset and show that there are still many open challenges to be addressed. The very high variability in video appearance between different surgeries becomes one of the major elements to consider while designing new approaches in this domain. This sets the motivation for organizing the FetReg challenge and push the boundaries of the current state-of-the-art.

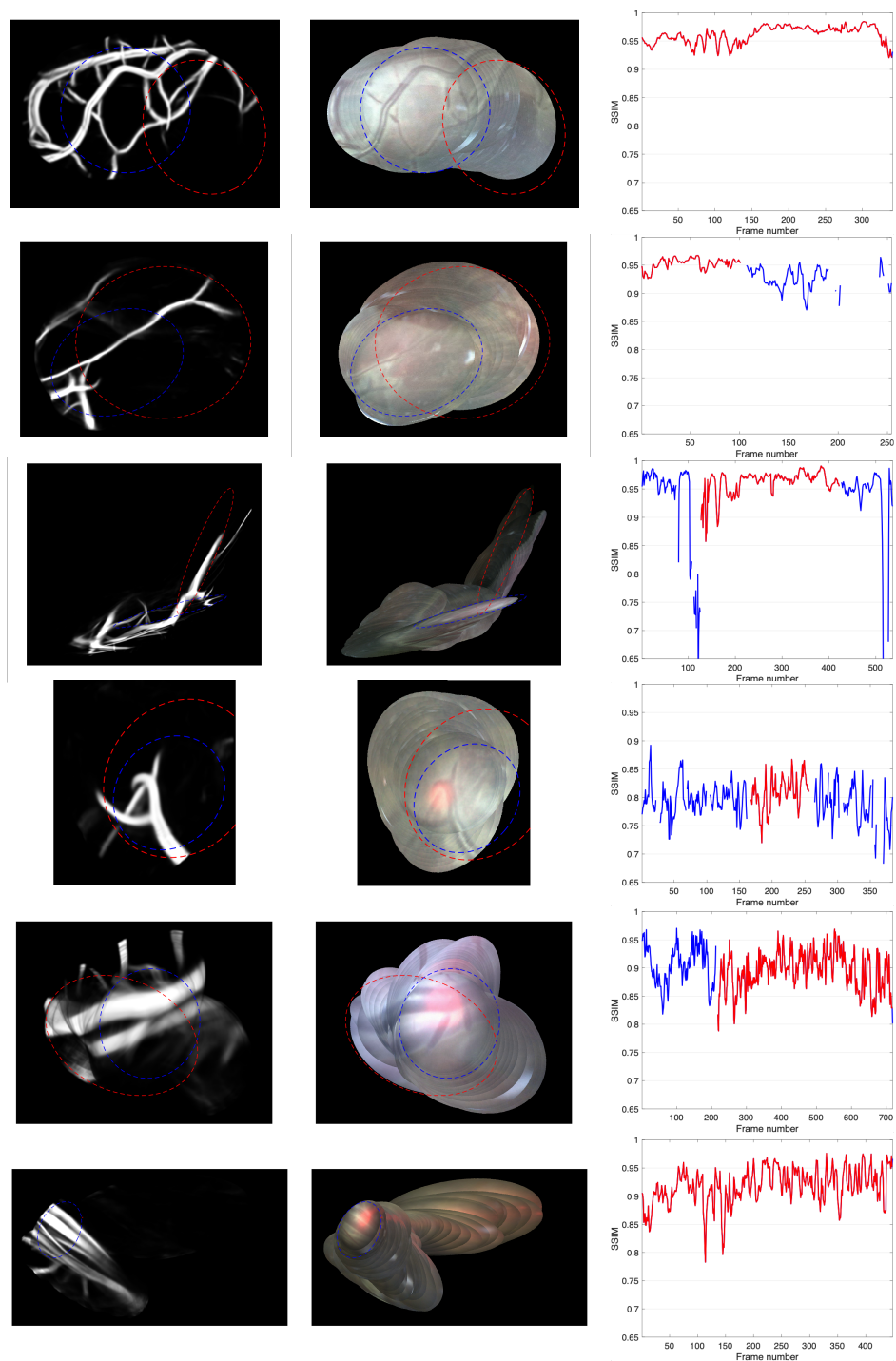


Figure 4: Left and centre show mosaics of vessel segmentations and RGB images respectively. Right shows the evaluation metric for every pair of images 5 frames apart in a sequence. Red represents the portion of frames visualized in the mosaics, while blue represents the remaining frames not shown in the mosaics. From top to bottom: Video001, Video002, Video003, Video004, Video005, Video006.

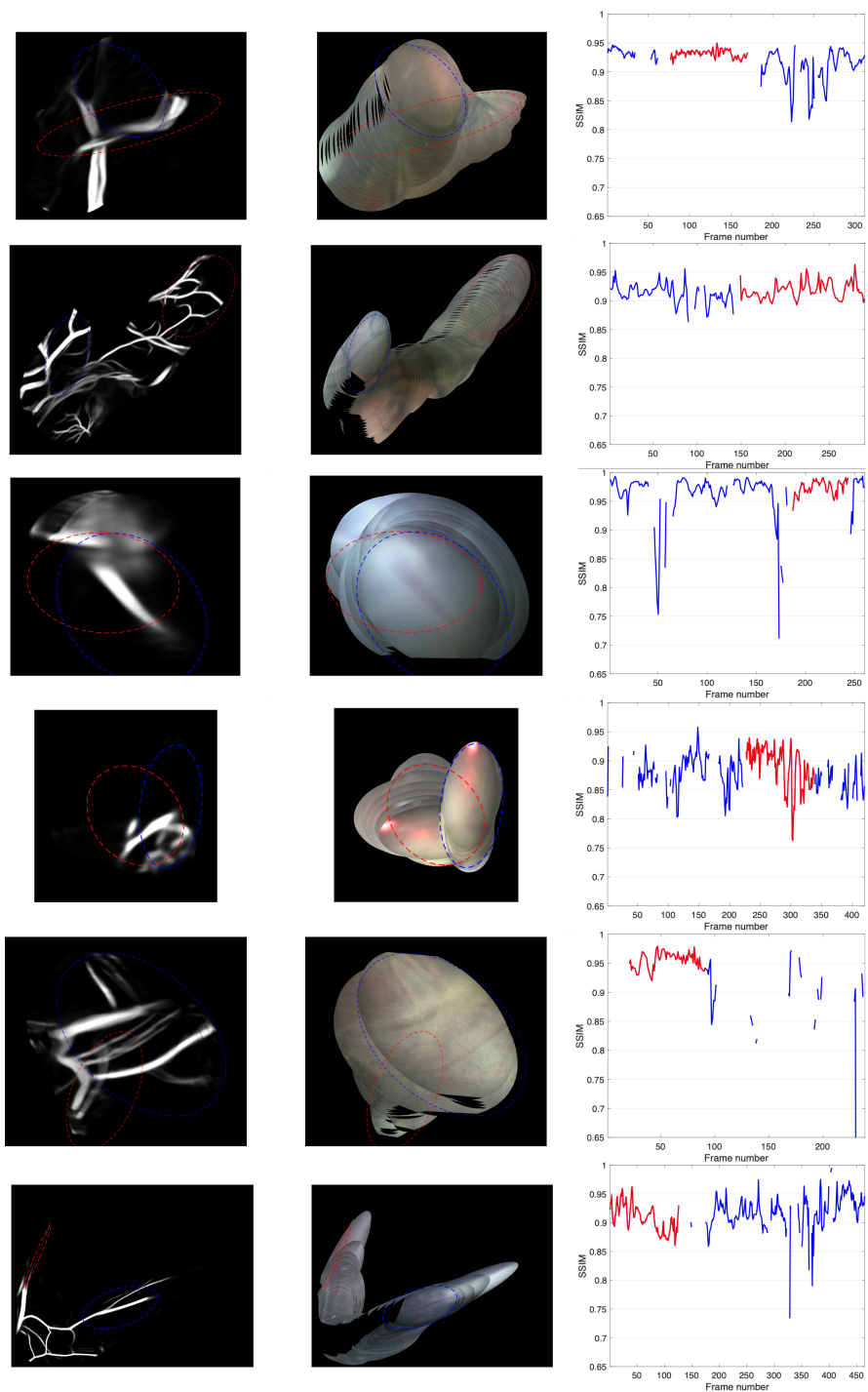


Figure 5: Left and centre show mosaics of vessel segmentations and RGB images respectively. Right shows the evaluation metric for every pair of images 5 frames apart in a sequence. Red represents the portion of frames visualized in the mosaics, while blue represents the remaining frames not shown in the mosaics. From top to bottom: Video007, Video008, Video009, Video011, Video013, Video014.

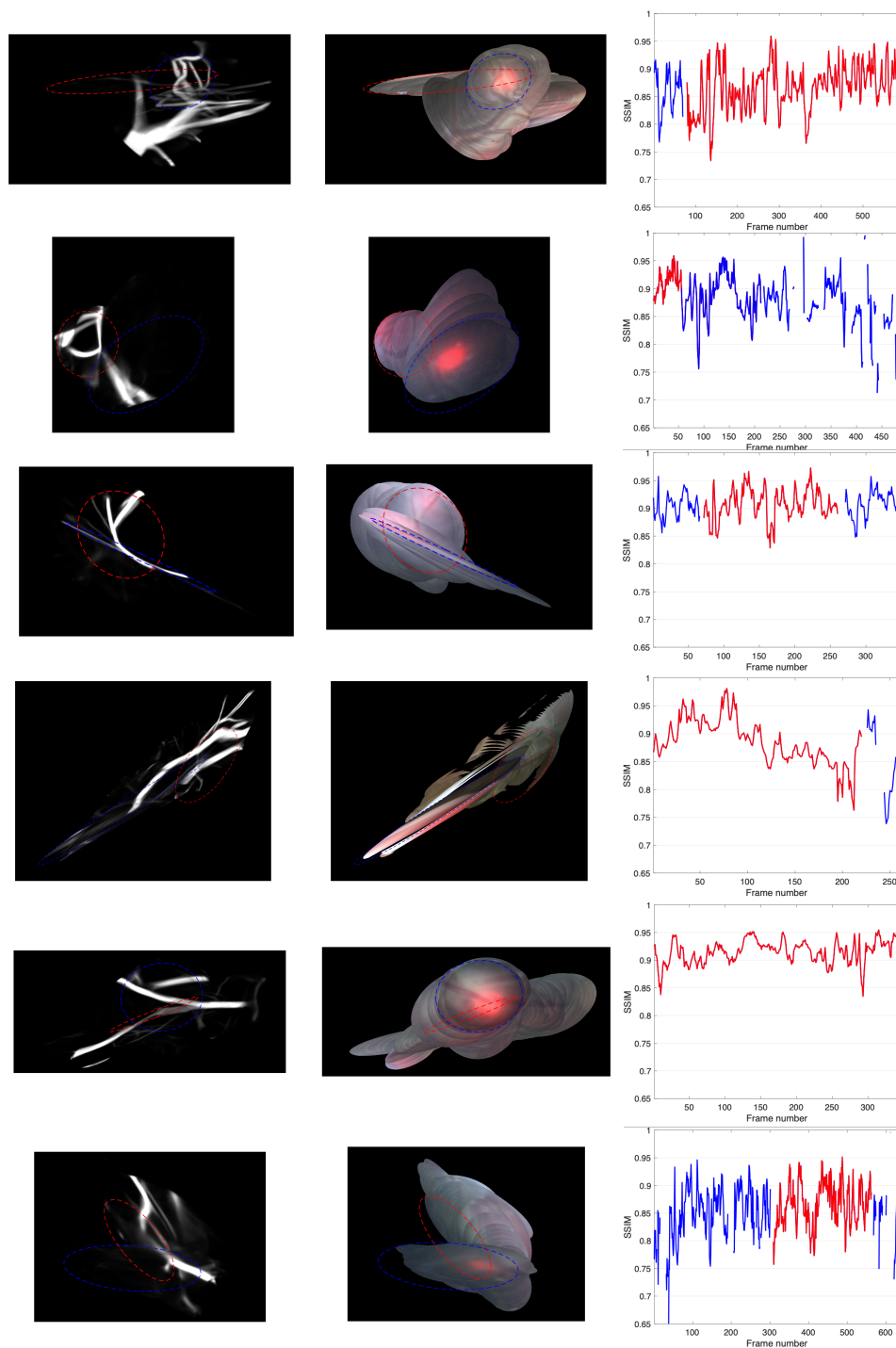


Figure 6: Left and centre show mosaics of vessel segmentations and RGB images respectively. Right shows the evaluation metric for every pair of images 5 frames apart in a sequence. Red represents the portion of frames visualized in the mosaics, while blue represents the remaining frames not shown in the mosaics. From top to bottom: Video016, Video017, Video018, Video019, Video022, Video023.

References

- [1] Ahmet Baschat, Ramen H. Chmait, Jan Deprest, Eduard Gratacós, Kurt Hecher, Efficia Kontopoulos, Ruben Quintero, Daniel W. Skupski, Dan V. Valsky, and Yves Ville. Twin-to-twin transfusion syndrome (TTTS). *Journal of Perinatal Medicine*, 39(2):107–112, 3 2011.
- [2] Liesbeth Lewi, Jan Deprest, and Kurt Hecher. The vascular anastomoses in monochorionic twin pregnancies and their clinical consequences, 1 2013.
- [3] Marie-Victoire Senat, Jan Deprest, Michel Boulvain, Alain Paupe, Norbert Winer, and Yves Ville. Endoscopic Laser Surgery versus Serial Amnioreduction for Severe Twin-to-Twin Transfusion Syndrome. *New England Journal of Medicine*, 351(2):136–144, 7 2004.
- [4] David Baud, Rory Windrim, Johannes Keunen, Edmond N. Kelly, Prakesh Shah, Tim Van Mieghem, P. Gareth R. Seaward, and Greg Ryan. Fetoscopic laser therapy for twin-twin transfusion syndrome before 17 and after 26 weeks' gestation. *American Journal of Obstetrics and Gynecology*, 208(3):1–197, 2013.
- [5] L. J. Salomon and Y. Ville. [Twin-to-twin transfusion syndrome: diagnosis and treatment]. *Bull Acad Natl Med*, 192(8):1575–1586, Nov 2008.
- [6] Christopher S. Muratore, Stephen R. Carr, Liesbeth Lewi, Roland Delieger, Marshall Carpenter, Jacques Jani, Jan A. Deprest, and Francois I. Luks. Survival after laser surgery for twin-to-twin transfusion syndrome: when are they out of the woods? *Journal of Pediatric Surgery*, 44(1):66–70, January 2009.
- [7] Jan A. Deprest, Alan W. Flake, Eduard Gratacos, Yves Ville, Kurt Hecher, Kypros Nicolaidis, Mark P. Johnson, François I. Luks, N. Scott Adzick, and Michael R. Harrison. The making of fetal surgery, 2010.
- [8] Rubén A. Quintero, Keisuke Ishii, Ramen H. Chmait, Patricia W. Bornick, Mary H. Allen, and Eftichia V. Kontopoulos. Sequential selective laser photocoagulation of communicating vessels in twin-twin transfusion syndrome. *Journal of Maternal-Fetal and Neonatal Medicine*, 20(10):763–768, 2007.
- [9] Masahiko Nakata, Takeshi Murakoshi, Haruhiko Sago, Keisuke Ishii, Yuichiro Takahashi, Satoshi Hayashi, Susumu Murata, Ichiro Miwa, Masahiro Sumie, and Norihiro Sugino. Modified sequential laser photocoagulation of placental communicating vessels for twin–twin transfusion syndrome to prevent fetal demise of the donor twin. *Journal of Obstetrics and Gynaecology Research*, 35(4):640–647, 2009.
- [10] Femke Slaghekke and Dick Oepkes. Solomon technique versus selective coagulation for twin–twin transfusion syndrome. *Twin Research and Human Genetics*, 19(3):217–221, 5 2016.
- [11] Robert Cincotta and Sailesh Kumar. Future Directions in the Management of Twin-to-Twin Transfusion Syndrome. *Twin Research and Human Genetics*, 19(3):285–291, 6 2016.
- [12] E. Lopriore, J. M. Middeldorp, D. Oepkes, F. J. Klumper, F. J. Walther, and F. P.H.A. Vandenbussche. Residual Anastomoses After Fetoscopic Laser Surgery in Twin-to-Twin Transfusion Syndrome: Frequency, Associated Risks and Outcome. *Placenta*, 28(2-3):204–208, 2 2007.
- [13] Rosalind Pratt, Jan Deprest, Tom Vercauteren, Sebastien Ourselin, and Anna L. David. Computer-assisted surgical planning and intraoperative guidance in fetal surgery: A systematic review, 12 2015.
- [14] Lena Maier-Hein, Swaroop S Vedula, Stefanie Speidel, Nassir Navab, Ron Kikinis, Adrian Park, Matthias Eisenmann, Hubertus Feussner, Germain Forestier, Stamatia Giannarou, et al. Surgical data science for next-generation interventions. *Nature Biomedical Engineering*, 1(9):691–696, 2017.
- [15] Alessandro Casella, Sara Moccia, Emanuele Frontoni, Dario Paladini, Elena De Momi, and Leonardo S Mattos. Inter-foetus membrane segmentation for TTTS using adversarial networks. *Annals of biomedical engineering*, 48(2):848–859, 2020.
- [16] Alessandro Casella, Sara Moccia, Dario Paladini, Emanuele Frontoni, Elena De Momi, and Leonardo S Mattos. A shape-constraint adversarial framework with instance-normalized spatio-temporal features for inter-fetal membrane segmentation. *Medical Image Analysis*, 70:102008, 2021.

- [17] Praneeth Satta, Metehan Imamoglu, Michael Dombrowski, Xenophon Papademetris, Mert O Bahtiyar, and John Onofrey. Deep-learned placental vessel segmentation for intraoperative video enhancement in fetoscopic surgery. *International Journal of Computer Assisted Radiology and Surgery*, 14(2):227–235, 2019.
- [18] Sophia Bano, Francisco Vasconcelos, Marcel Tella Amo, George Dwyer, Caspar Gruijthuijsen, Jan Deprest, Sebastien Ourselin, Emmanuel Vander Poorten, Tom Vercauteren, and Danail Stoyanov. Deep sequential mosaicking of fetoscopic videos. In *International Conference on Medical Image Computing and Computer-Assisted Intervention*, pages 311–319. Springer, 2019.
- [19] Sophia Bano, Francisco Vasconcelos, Luke M Shepherd, Emmanuel Vander Poorten, Tom Vercauteren, Sebastien Ourselin, Anna L David, Jan Deprest, and Danail Stoyanov. Deep placental vessel segmentation for fetoscopic mosaicking. In *International Conference on Medical Image Computing and Computer-Assisted Intervention*, pages 763–773. Springer, 2020.
- [20] Marcel Tella-Amo, Loïc Peter, Dzhoshkun I Shakir, Jan Deprest, Danail Stoyanov, Tom Vercauteren, and Sebastien Ourselin. Pruning strategies for efficient online globally consistent mosaicking in fetoscopy. *Journal of Medical Imaging*, 6(3):035001, 2019.
- [21] Pankaj Daga, François Chadebecq, Dzhoshkun I Shakir, Luis Carlos Garcia-Peraza Herrera, Marcel Tella, George Dwyer, Anna L David, Jan Deprest, Danail Stoyanov, Tom Vercauteren, et al. Real-time mosaicing of fetoscopic videos using SIFT. In *Medical Imaging 2016: Image-Guided Procedures, Robotic Interventions, and Modeling*, volume 9786, page 97861R. International Society for Optics and Photonics, 2016.
- [22] Mireille Reeff, Friederike Gerhard, Philippe Cattin, and Székely Gábor. Mosaicing of endoscopic placenta images. *INFORMATIK 2006—Informatik für Menschen, Band 1*, 2006.
- [23] Loïc Peter, Marcel Tella-Amo, Dzhoshkun Ismail Shakir, George Attilakos, Ruwan Wimalasundera, Jan Deprest, Sébastien Ourselin, and Tom Vercauteren. Retrieval and registration of long-range overlapping frames for scalable mosaicking of in vivo fetoscopy. *International Journal of Computer Assisted Radiology and Surgery*, 13(5):713–720, 2018.
- [24] Floris Gaisser, Suzanne HP Peeters, Boris AJ Lenseigne, Pieter P Jonker, and Dick Oepkes. Stable image registration for in-vivo fetoscopic panorama reconstruction. *Journal of Imaging*, 4(1):24, 2018.
- [25] George Dwyer, Francois Chadebecq, Marcel Tella Amo, Christos Bergeles, Efthymios Maneas, Vijay Pawar, Emanuel Vander Poorten, Jan Deprest, Sebastien Ourselin, Paolo De Coppi, et al. A continuum robot and control interface for surgical assist in fetoscopic interventions. *IEEE robotics and automation letters*, 2(3):1656–1663, 2017.
- [26] George Dwyer, Richard J Colchester, Erwin J Alles, Efthymios Maneas, Sebastien Ourselin, Tom Vercauteren, Jan Deprest, Emmanuel Vander Poorten, Paolo De Coppi, Adrien E Desjardins, et al. Robotic control of a multi-modal rigid endoscope combining optical imaging with all-optical ultrasound. In *2019 International Conference on Robotics and Automation (ICRA)*, pages 3882–3888. IEEE, 2019.
- [27] Sophia Bano, Francisco Vasconcelos, Marcel Tella-Amo, George Dwyer, Caspar Gruijthuijsen, Emmanuel Vander Poorten, Tom Vercauteren, Sebastien Ourselin, Jan Deprest, and Danail Stoyanov. Deep learning-based fetoscopic mosaicking for field-of-view expansion. *International Journal of Computer Assisted Radiology and Surgery*, 15(11):1807–1816, 2020.
- [28] Sophia Bano, Francisco Vasconcelos, Emmanuel Vander Poorten, Tom Vercauteren, Sebastien Ourselin, Jan Deprest, and Danail Stoyanov. Fetnet: a recurrent convolutional network for occlusion identification in fetoscopic videos. *International journal of computer assisted radiology and surgery*, 15(5):791–801, 2020.
- [29] Olaf Ronneberger, Philipp Fischer, and Thomas Brox. U-net: Convolutional networks for biomedical image segmentation. In *International Conference on Medical image computing and computer-assisted intervention*, pages 234–241. Springer, 2015.
- [30] Kaiming He, Xiangyu Zhang, Shaoqing Ren, and Jian Sun. Deep residual learning for image recognition. In *Proceedings of the IEEE conference on computer vision and pattern recognition*, pages 770–778, 2016.